H.R. SHARMA,[1] S. NAGU,[2] J. SINGH,[2] R.B. SINGH,[2] B. POTUKUCHI[1]

[1] Department of Physics, University of Jammu
 (Jammu Tawi-180006, Jammu, India; e-mail: hansraj77sharma@gmail.com)
[2] Department of Physics, University of Lucknow
 (Lucknow, India)

QUANTIFYING EFFECTS
OF FINAL-STATE INTERACTIONS
ON ENERGY RECONSTRUCTION IN DUNE

In neutrino-nucleus interactions, the particles produced at the primary vertex may be different from the particles observed in the final state. This is due to the effect of final-state interactions (FSI) on the particles during their transport in the nuclear matter to reach the detector (final state) after their production at the primary vertex. In this report, the energy reconstruction is done for charged current quasielastic (CCQE) and charged current resonance (CCRES) scatterings on the event-by-event basis using the calorimetric method, and NuWro and GENIE simulation tools. In addition, the percentage of fake events in CCQE and CCRES interactions is presented. It is found that the percentage of fake events is more than 50% for both CCQE and CCRES processes for both the generators, if we apply the condition for the signal events that the particles observed in the final state should be the same as the particles produced at the primary vertex. Based on our definition of signal events, the reconstructed energy and number of fake events may change, and this influences the measurement of oscillation parameters in long-baseline experiments like DUNE.

K e y w o r d s: final state interactions, DUNE, fake events, energy reconstruction.

1. Introduction

Neutrinos interact with matter through the charged current (CC) and neutral current (NC) weak interactions by the exchange of $W^{\pm}$ and Z^0 bosons. The interactions and properties of neutrinos are being studied to explore physics beyond the standard model. In its earlier formalism, the standard model assumed the neutrinos to be massless. The phenomenal experiments done recently have made sensational discoveries in the field of neutrino oscillations – a phenomenon wherein a neutrino of a specific flavor can later be observed to have a different flavor [1], and, for that, neutrinos should have mass. Neutrino oscillation physics is handled by neutrino oscillation parameters – mixing angles $(\theta_{12}, \theta_{13}, \theta_{23})$, Dirac phase δ_{cp}, and magnitude of mass squared differences Δm_{21}^2 (solar mass splitting) and Δm_{32}^2 (atmospheric mass splitting) [2]. The almost precise determination of mixing angles θ_{12}, θ_{23} and non-zero value of θ_{13} and mass

squared differences Δm_{21}^2, $|\Delta m_{32}^2|$ have been made [3–6]. But still, there are some unknown parameters:

1) the neutrino mass ordering, i.e., the sign of Δm_{32}^2. In the normal mass hierarchy (NH), the neutrino mass ordering is $m_1 \ll m_2 \ll m_3$, and for the inverted mass hierarchy (IH), the neutrino mass ordering is $m_1 \approx m_2 \gg m_3$.

2) determination of octant of θ_{23}, i.e., to find out whether θ_{23} lies in the lower octant (LO) $0 < \theta_{23} < \frac{\pi}{4}$ or higher octant (HO) $\frac{\pi}{4} < \theta_{23} < \frac{\pi}{2}$.

3) Dirac phase parameter δ_{cp} which may lie in the range $-\pi < \delta_{cp} < \pi$. CP violation in the leptonic sector would be indicated, if the value of δ_{cp} differs from 0 or π.

The Deep Underground Neutrino Experiment (DUNE) [7–10], one of the long-baseline future neutrino experiments in the USA, is being designed to solve some fundamental problems in neutrino physics. It has a near detector (ND) system located at Fermilab and a far detector (FD) system located nearly 1300 km away from Fermilab at South Dakota. The three primary components of the DUNE
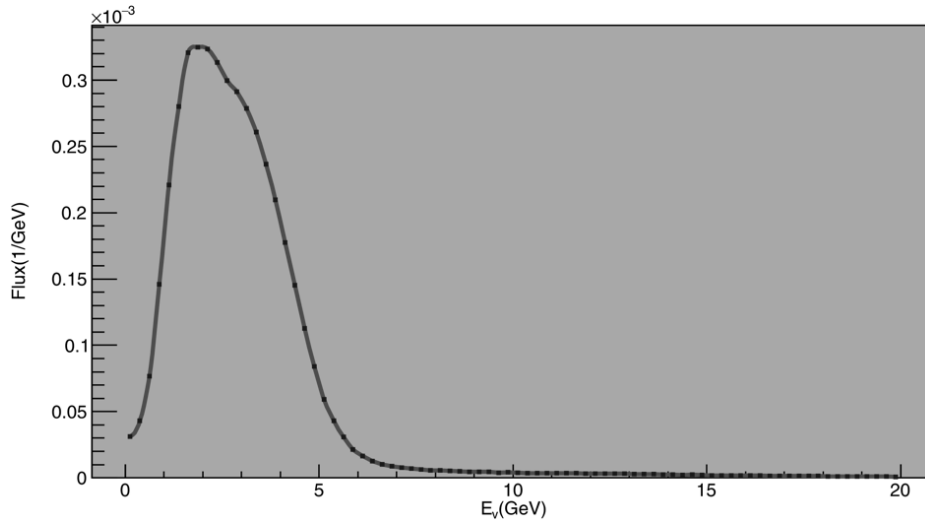
Fig. 1. DUNE flux used in our work

ND system are: 1) A 50-ton LArTPC (ND-LAr) constructed using ArgonCube. 2) A multi-purpose detector (MPD) called ND-GAr detector that consists of high pressure-gaseous argon TPC surrounded by an electromagnetic calorimeter, and 3) an on-axis beam monitor called System for on-Axis Neutrino Detection (SAND) monitors the flux of neutrinos. The DUNE far detector (FD) will be made of four similar LArT-PCs, each will have a fiducial mass of at least 10 kt, installed 1.5 km underground. Each LAr TPC module will be installed in a cryostat (at a temperature of 88 K) with internal dimensions 15.1 m (w) × × 14.0 m (h) × 62.0 m(l). The DUNE FD will be able to exceptionally reconstruct neutrino interactions with image-like precision and outstanding resolution. The significant problems that DUNE aims to inspect are the neutrino mass hierarchy, determination of CP violation phase, and octant degeneracy.

In our simulation work, the DUNE flux [11] (energy range 0.125–19.975 GeV), and argon (Ar, $Z =$ $= 18$, $A = 40$) nuclei (as target) have been used (Fig. 1). The flux peaks around 2.5 GeV and covers the energy spectrum from around 100 MeV to tens of GeV. An intense neutrino beam, provided by NuMI (Neutrino at Main Injector) beamline facility at Fermilab, will aim at DUNE detectors. ND will observe the unoscillated neutrino spectrum, and FD will observe the oscillated neutrino spectrum. The study of systematic uncertainties is required to achieve the goals of DUNE up to the desired extent.

In neutrino experiments, the use of heavy targets (like Ar) will give large event statistics, but will boost the nuclear effects. This reduces the statistical errors, but shifts the attention toward the sources of systematic errors. Uncertainties in the determination of neutrino-nucleus cross-sections which arise due to the presence of nuclear effects are one of the most important sources of systematic errors. Uncertainties in neutrino-nucleus cross-sections and their effects on the determination of neutrino oscillation parameters have been discussed in many previous works [12–14]. The current knowledge of nuclear effects is still insufficient to have good control over systematic errors produced due to nuclear effects [15–18]. The major nuclear effects present in nuclear targets are nuclear Fermi motion effects, uncertainties from nuclear binding energy, multi-nuclear correlation, and final-state interactions (FSI) of hadrons produced.

As the neutrino oscillation probability itself depends on the energy of neutrinos, the correct reconstruction of the neutrino energy is essential in the study of neutrino oscillations [19]. Neutrino energy, if reconstructed incorrectly, causes uncertainties in the cross-section measurement and event identification. These uncertainties will be propagated to the measurement of neutrino oscillation parameters. The neutrino beams obtained from accelerators, used in most of the long-baseline neutrino oscillation experiments, are not mono-energetic, and, thus, a com-

plete knowledge of final-state particles produced in neutrino interactions is required for the correct measurement of the neutrino energy, as the detectors capture the final-state particles. But, because of nuclear effects, these particles are different (or not identical) from the particles produced at the primary vertex. Thus, it is necessary to have the complete knowledge of nuclear effects and final-state interactions for the correct reconstruction of the neutrino energy.

In this work, we have used the calorimetric method for the energy reconstruction for QE and RES events in the DUNE experimental setup using NuWro (version 19.2.2) and GENIE (version 3.0.6) event generators. We have also shown the percentage of fake events present in QE and RES interactions. This work is organized into the following sections: Section 2 contains the description of NuWro and GENIE generators. Section 3 contains a brief discussion of charged current neutrino interactions. In Section 4, methods of energy reconstruction are discussed. Results of the simulation are given in Section 5 followed by a summary in Section 6.

2. NuWro and GENIE Monte Carlo Generators

Neutrino event generators are used in the analysis of experimental data, the design and optimization of detectors, and the evaluation of systematic errors for measurements. These Monte Carlo generators involve detector specifications to perform the simulation for any experiment to get an idea of the expected observables. We have used version 19.2.2 of NuWro and version 3.0.6 of GENIE. These generators

Table 1. **Models used by NuWro and GENIE Monte Carlo generators**

Process/Model	Models used by NuWro	Models Used by GENIE
QE	Llewellyn Smith model	Llewellyn Smith model
RES	Adler–Rarita–Schwinger model	Rein–Sehgal model
Nuclear model	Local Fermi Gas Model	Relativistic Fermi Gas Model
FSI model	Intra-nuclear Cascade	INTRANUKE hA 2018

are being used by many neutrino experiments in the world. Recently, the T2K experiment used NuWro in the estimation of systematic errors, while the MINERvA experiment used it in the measurement of flux-averaged differential cross-section and two-body current distribution. GENIE is being used by many neutrino baseline experiments, such as MINERvA [20], MINOS [21], MicroBOONE [22], NOvA [23], and T2K [24]. DUNE is also using GENIE for the simulation.

Both NuWro and GENIE are written in C++ language. NuWro is simple to handle and contains a text file "params.txt" in which all simulation parameters can be fitted. NuWro is more theory-oriented and is recently developed by a group of theoreticians at Wroclaw University. It can simulate neutrino interactions for all neutrino flavors and all targets over the energy range from few MeV to TeV for scattering off a free nucleon. GENIE is the most sophisticated and modern package developed by the international collaboration for ongoing neutrino oscillation experiments and can be used to simulate neutrino interactions for all neutrino flavors and all targets over the energy range from the threshold to hundreds of GeV.

In NuWro, the local Fermi gas model, global Fermi gas model, and spectral functions are used as nuclear models, while, in GENIE, the relativistic Fermi gas model, based on the model suggested by A. Bodek and J.L. Ritchie [25] is used. The local Fermi gas model and spectral functions can also be used as nuclear models in GENIE. Both NuWro and GENIE use the Llewellyn Smith model [26] for describing the QE scattering. The latest BBBA05 [27] vector form factor is used by NuWro, while the latest BBBA07 [28] vector form factor is used by GENIE. For RES interactions, NuWro uses the Adler–Rarita–Schwinger model [29], while GENIE uses the Rein–Sehgal model [30]. Intranuclear hadron transport in NuWro is handled by its own intranuclear cascade model, while GENIE uses a sub package called INTRANUKE for the re-scattering of pions and nucleons in the nucleus. In NuWro, we use variable values of the axial mass between 0.94–1.03 GeV/c^2. In GENIE, we use variable values of the axial mass (M_A) between 0.99–1.2 GeV/c^2. In our simulation, we have used $M_A^{\text{QE}} = 0.99$ GeV/c^2 and $M_A^{\text{RES}} = 1.12$ GeV/c^2 for both NuWro and GENIE. Table 1 shows the models used in NuWro and GENIE generators for various processes in our simulation.

3. Neutrino-Nucleus Interactions

Neutrinos undergo weak interactions with the matter by the exchange of $W^{\pm}$ or Z^0 bosons. We can classify neutrino interactions into two main categories: charged current (CC) neutrino interactions (exchange particle is $W^{\pm}$) and neutral current (NC) neutrino interactions (exchange particle is Z^0):

$$\nu_l + N \longrightarrow l^- + X, \quad \bar{\nu}_l + N \longrightarrow l^+ + X, \text{ CC}, \quad (1)$$

$$\nu_l + N \longrightarrow \nu_l + N, \quad \bar{\nu}_l + N \longrightarrow \bar{\nu}_l + N, \text{ NC}. \quad (2)$$

where $N = n$, p or a target (with given protons and neutrons), $l = e$, μ or τ, and $X =$ the hadronic final state.

The exchange of W bosons involves a transfer of electric charge. So, the interaction is known as the "charged current (CC) interaction". In contrast, the exchange of Z bosons involves no transfer of electrical charge and is referred as "neutral current (NC) interaction".

Each CC or NC interaction is further classified into the following main categories:

1. *Quasielastic and Elastic Scatterings.* The neutrino may scatter off the nucleon with the ejection of the nucleon from the target. For charged current events, the scattering is quasielastic, and, for neutral current events, the scattering is elastic. For muon neutrinos, the interactions may be written as:

$$\nu_\mu + n \longrightarrow \mu^- + p, \quad \bar{\nu}_\mu + p \longrightarrow \mu^+ + n, \quad (3)$$

$$\nu_\mu(\bar{\nu}_\mu) + n \longrightarrow \nu_\mu(\bar{\nu}_\mu) + n,$$
$$\nu_\mu(\bar{\nu}_\mu) + p \longrightarrow \nu_\mu(\bar{\nu}_\mu) + p. \quad (4)$$

2. *Resonance Production.* The neutrino may excite the target nucleon to a resonance state which then usually decays into a nucleon and a single pion. For muon neutrinos, the interactions are:

$$\nu_\mu + N \longrightarrow \mu^- + N^* \longrightarrow \mu^- + \pi + N', \quad (5)$$

$$\bar{\nu}_\mu + N \longrightarrow \mu^+ + N^* \longrightarrow \mu^+ + \pi + N'. \quad (6)$$

Here, N, $N' = n$ or p; $\pi = \pi^+$, π^- or π^0; N^* is a resonance state, mostly Δ (1232) resonance is produced, but the production of other higher resonances is also possible. These interactions can occur for both CC and NC processes.

3. *Deep Inelastic Scattering (DIS):* In this type of scattering, a high-energy neutrino scatters off a quark in the nucleon via the exchange of W or Z boson producing a lepton and a hadronic system (shower) [31]. The interactions can occur for both CC and NC processes.

4. *Coherent Scattering.* Neutrinos can scatter off from the nucleus as a whole coherently, thereby producing a lepton and a pion. The contribution to the pion production by this process is small.

5. *2p-2h Scattering Process.* In 2p-2h interactions (also called as meson exchange (MEC) interactions), an incoming neutrino interacts with a correlated pair of nucleons in the nucleus and transfers the energy and momentum to the nucleons, ejecting two nucleons from the nucleus. These 2p-2h events are also called MEC (meson exchange) events, as, in the initial stage, nucleons keep on exchanging a pion between them. 2p-2h events are high-energy cross-section QE-like events [32, 33] and mostly appear in the region between QE and RES production. The experimental signature of this interaction is $1\mu^-$ and no pion which is the same as for true QE interaction or RES interaction with a pion absorbed in the nuclear matter.

4. Energy Reconstruction

In neutrino oscillation experiments, the oscillation probability depends on true neutrino energy, (E_ν^{true}) [34], and these experiments must determine the neutrino energy from the lepton kinematics and the hadronic information from charged current (CC) neutrino interactions. The energy reconstructed (E_ν^{reco}) by any method must account for any unobserved energy deposition, incorporating particles below the detection threshold, escaping neutral particles, and inactive material. Practically, the assumptions about these effects are based on the cross-section model. The uncertainties induced by nuclear effects make the energy reconstruction a challenging task. It is not possible to isolate the nuclear effects as neutrino beams to be used have a broader energy distribution than the nuclear effects of interest. Generally, it is not possible to measure the entire outgoing state (particularly, the struck nucleus), and, thus, the momentum transfer in the neutrino scattering is basically unknown. The strong interactions alter the composition and kinematics of final-state particles and the determination of incident neutrino energy. The reconstructed energy also depends on the detector technology, as low-energy particles may escape the detection depending on the detection threshold of the detector. The energy reconstruction is to be done on

the event-by-event basis, as the neutrinos in the generated neutrino beams have a broad range of energies. Two methods of energy reconstruction of neutrinos are 1. Kinematic Method and 2. Calorimetric Method [35, 36].

In case, if a single nucleon is emitted in a neutrino interaction, the neutrino energy is given by:

$$E_\nu^{\text{kin}} = \frac{2(M - \epsilon)E_l + M^2 - (M - \epsilon)^2 - m_l^2}{2(M - \epsilon - E_l + |k_l| \cos\theta)}. \quad (7)$$

Here, M is the mass of the emitted nucleon, ϵ is a single-nucleon separation energy, m_l, E_l, and k_l are the mass, energy, and momentum of the outgoing charged lepton, θ is the angle between the directions of the beam and the outgoing lepton. This method of reconstruction is known as the "kinematic method" and works, if the true nature of the event is a CCQE process. The method is based on assumptions that the neutrino in the beam interacts with a single nucleon which is at rest and bound with constant energy. The energy estimation given by relation (7) is very far from true energy for non-CCQE processes such as CC1π production followed by the pion absorption in the nuclear medium or 2p-2h processes. The same thing holds, if an extra meson is produced in the final state, and the meson is not detectable because of its low energy (below the detection threshold) or is not identified by a tracking software or is absorbed in the nuclear matter. In addition, this method assumes the single-nucleon separation energy ϵ as fixed. But in reality, the struck nucleon momentum is drawn from a target nucleus. The kinematic method of energy reconstruction is used in lower energy experiments. As the energy of incoming neutrinos increases, the contribution of RES and DIS processes increases. This increases the hadrons in the final state thereby leading to the wrong estimation of the neutrino energy. This method of energy reconstruction is used in lower energy experiments such as MiniBooNE and T2K [32, 37, 38]. These experiments use neutrino beams peaked at $E_\nu \approx 600$–800 MeV and determine the energy distribution of CC events from kinematics (i.e., KE and emission angle) of the outgoing charged lepton using large Cherenkov detectors filled with water or mineral oil.

In the energy regime well above 1 GeV, calorimeters provide an alternative to the Cherenkov detectors. Calorimeters measure the visible energy deposited by the final-state particles associated with each event. They were used in MINOS [39] and NOvA [40] experiments. In these experiments, the total energy deposited by all reaction products is measured without a prior reconstruction of the track, momentum, or energy of each final-state particle. For potentially complex final states, the energy response is calibrated using test-beam exposures. However, neutrino experiments like DUNE [41] are applying detectors capable of fine-grained tracking of a large number of interaction products, and this capability of these detectors is the key of being able to select electron-neutrino events and to distinguish them from backgrounds even for non-QE events. The calorimetric technique of energy reconstruction obviously depends on the ability to fully reconstruct the final state which mainly depends on the performance and design of the detector. The missing energy due to nuclear effects also hampers the energy reconstruction. For example, a pion absorbed in the nuclear matter after its production in the primary vertex would not deposit its energy in the calorimeter.

The neutrino reconstructed energy E_ν^{cal}, using the calorimetric method, for CC neutrino interactions resulting in the knockout of "n" nucleons and production of "m" mesons is given by:

$$E_\nu^{\text{cal}} = E_l + \epsilon_{\text{nucl}} + \sum_{i=1}^{n}(E_i - M) + \sum_{j=1}^{m} E_j, \quad (8)$$

where E_ν^{cal} is the calorimetric reconstructed neutrino energy, E_l is the energy of the outgoing lepton, ϵ_{nucl} is the single-nucleon separation energy (sum of the nucleon excitation energy and recoil energy of the nucleus) = 34 MeV, E_i is the energy of ith knocked out nucleon, M is the mass of a nucleon, E_j is the energy of jth produced meson.

The sensitivity of an experiment to the intranuclear rescattering depends on the energy range of neutrinos, the physics measurement being made, and the detector technology. The hadrons produced in the primary vertex usually undergo FSI during their propagation through the nucleus. Thus, the particles in the primary state are often different from the particles in the final state. For example, a QE interaction that emits a lepton and a proton can end up with a final state of one lepton, three protons, two neutrons, and a few photons with a finite probability. The wrong energy will be measured for these events, as the topology is often mistaken. Thus, to
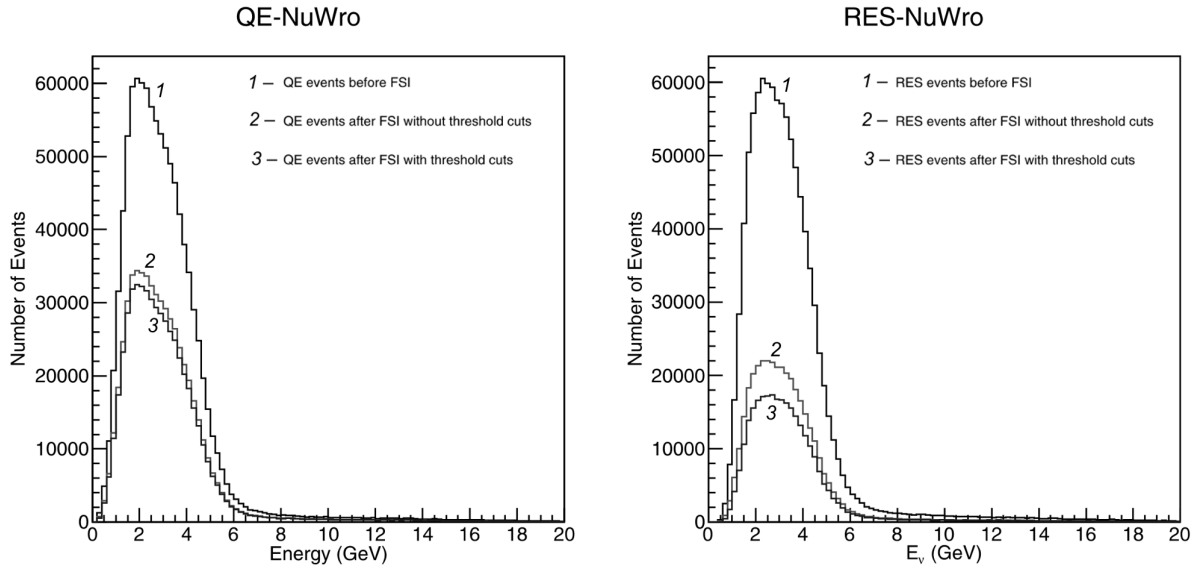
QE-NuWro

RES-NuWro

Fig. 2. Distribution of QE (left panel) and RES (right panel) events before FSI (lines *1*), after FSI without detection threshold cuts (lines *2*) and with kinetic energy detection threshold cuts (lines *3*), for NuWro generator. In the final state (after FSI), only that events are chosen as signal events which have $1\mu^-$ and exactly 1 proton for QE processes and $1\mu^-$, 1π and 1 nucleon for RES processes

understand the role of these events, a high-quality Monte Carlo code is required.

5. Results and Discussion

For both QE and RES processes, we have generated 1 million events using NuWro and GENIE generators. The energy reconstruction is done on the event-by-event basis using the calorimetric method (relation 8). Firstly, we define CCQE signal events as those having $1\mu^-$, no pions, and 1 proton in the final state and CCRES signal events as those having $1\mu^-$, 1 pion and exactly 1 nucleon in the final state, i.e., exactly that topology of particles which is for the primary vertex. The events which do not satisfy these conditions are called as fake events. The results on the reconstructed energy are shown in Fig. 2 for NuWro and in Fig. 3 for GENIE. In each figure, the black line represents the reconstructed energy at the primary vertex before FSI, the red line represents the reconstructed energy after FSI without detection threshold cuts, and the blue line represents the reconstructed energy with detection threshold cuts applied on the kinetic energy of the particles in the final state (after FSI). The values of kinetic energy detection threshold cuts are shown in Table 2 and are for DUNE detector [42]. It is clear from Fig. 2 and Fig. 3 that, for the

given condition on signal events (QE signal events are those having $1\mu^-$, no pions, and 1 proton in the final state and CCRES signal events as those having $1\mu^-$, 1 pion and exactly 1 nucleon in the final state), we are getting a lesser number of events as signal events in the final state. This is due to the fact that nuclear effects and FSI change the topology of the particles produced at the primary vertex during their intranuclear transport, before they reach the detector. The results for energy reconstruction are better for QE events, than for RES events for both the generators. The percentage of fake events are shown in Tables 3 and 4 for NuWro and GENIE, respectively. It is clear that the percentage of fake events is fairly above 50. Thus, in a very low number of events, the particles produced at the primary vertex reach the final state as such without undergoing FSI. Thus, FSI creates problems in

Table 2. **Detection thresholds for various final-state particles in DUNE**

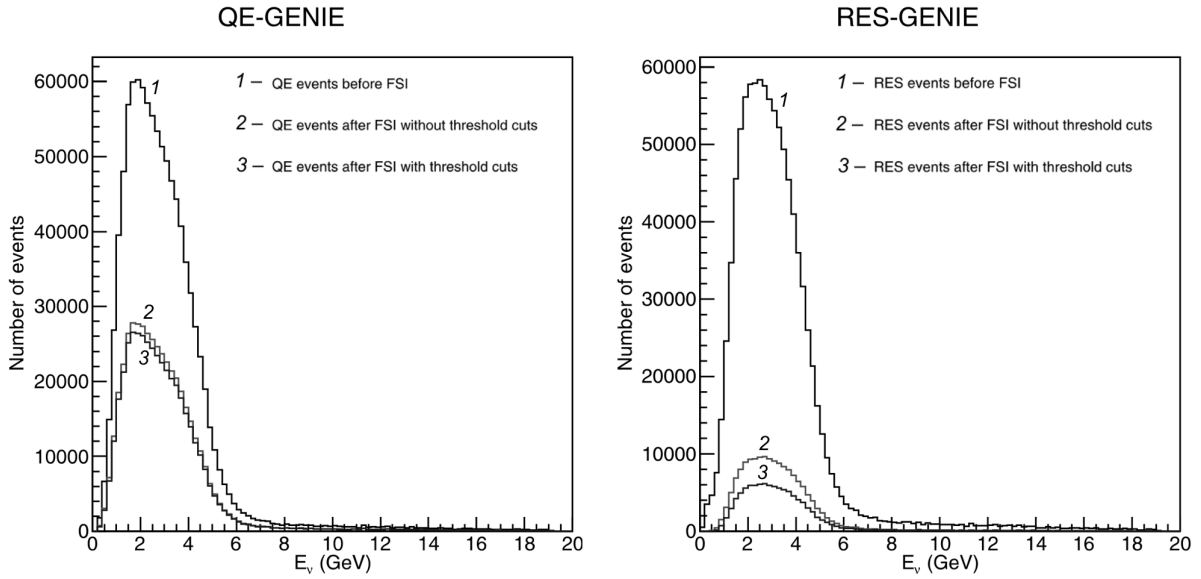| Particle type	KE detection threshold, MeV
$e^\pm$, $\mu^\pm$, γ	30
$\pi^\pm$	100
p, n, other	50

Fig. 3. Distribution of QE (left panel) and RES (right panel) events before FSI (lines *1*), after FSI without detection threshold cuts (lines *2*) and with kinetic energy detection threshold cuts (lines *3*), for GENIE generator. In the final state (after FSI), only that events are chosen as signal events which have $1\mu^-$ and exactly 1 proton for QE processes and $1\mu^-$, 1π and 1 nucleon for RES processes
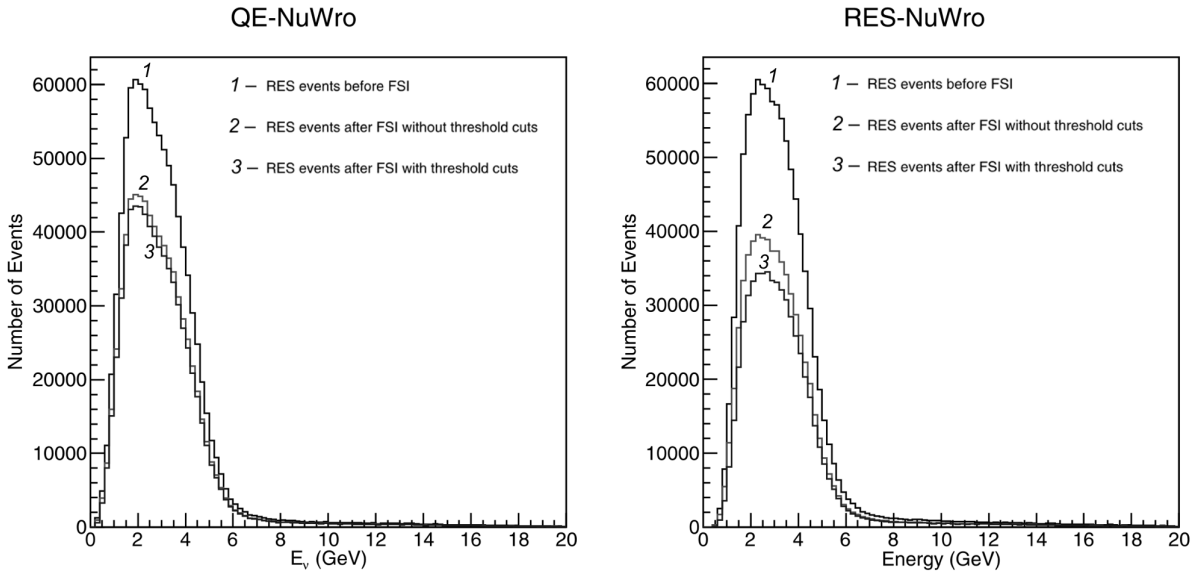

Fig. 4. Distribution of QE (left panel) and RES (right panel) events before FSI (lines *1*), after FSI without detection threshold cuts (lines *2*) and with kinetic energy detection threshold cuts (lines *3*), for NuWro generator. In the final state (after FSI), only that events are chosen as signal events which have $1\mu^-$, 0π, exactly 1 proton and X neutrons for QE processes and $1\mu^-$, 1π and X nucleons for RES processes

the correct estimation of the energy in neutrino experiments. In addition, detector thresholds increase the percentage of fake events and are to be minimized for the correct reconstruction of neutrino energies.

Now, we define CCQE signal events as those having $1\mu^-$, 0π, exactly 1 proton and X neutrons in the final state and CCRES signal events as those having $1\mu^-$, exactly 1π and X nucleons in
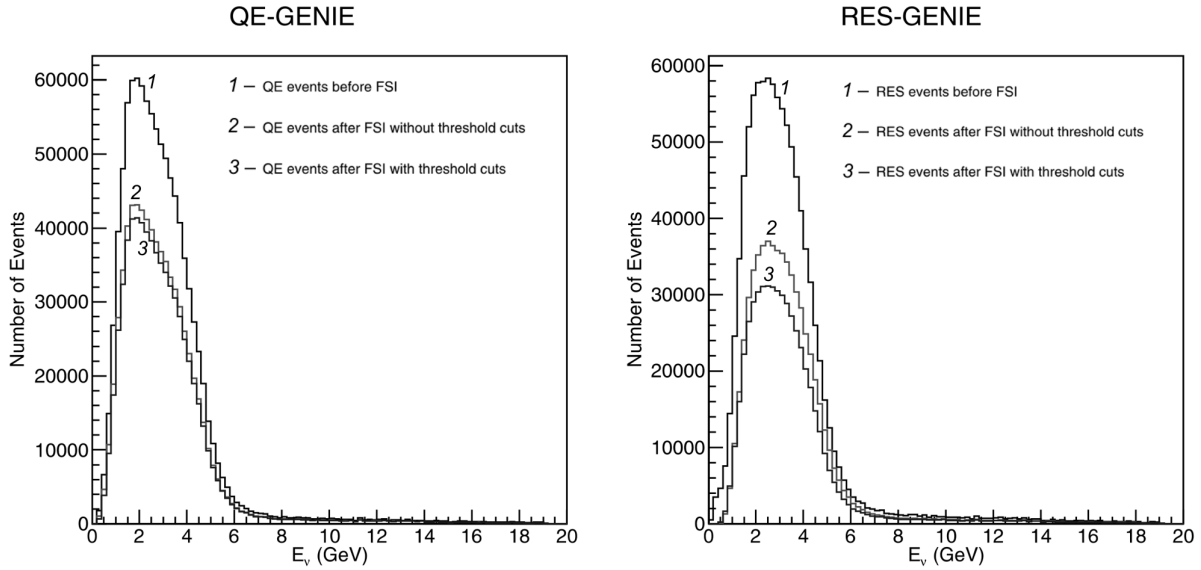
Fig. 5. Distribution of QE (left panel) and RES (right panel) events before FSI (lines *1*), after FSI without detection threshold cuts (lines *2*) and with kinetic energy detection threshold cuts (lines *3*), for GENIE generator. In the final state (after FSI), only that events are chosen as signal events which have $1\mu^-$, 0π, exactly 1 proton and X neutrons for QE processes and $1\mu^-$, 1π and X nucleons for RES processes

Table 3. **Percentage of fake events in NuWro, calculated as a difference of total number of events before FSI and after FSI with condition on QE events as having $1\mu^-$, 0π and 1 proton in the final state and the condition on RES events as having $1\mu^-$, 1π, and 1 nucleon in the final state**

Interaction type	% age of fake events without cuts	% age of fake events with cuts
QE	43	46
RES	63	71

Table 4. **Percentage of fake events in GENIE, calculated as a difference of the total number of events before FSI and after FSI with condition on QE events as having $1\mu^-$, 0π and 1 proton in the final state and condition on RES events as having $1\mu^-$, 1π, and 1 nucleon in the final state**

Interaction type	% age of fake events without cuts	% age of fake events with cuts
QE	54	56
RES	83	89

Table 5. **Percentage of fake events in NuWro, calculated as a difference of the total number of events before FSI and after FSI with condition on QE events as having $1\mu^-$, 0π, 1 proton and X neutrons in the final state and condition on RES events as having $1\mu^-$, 1π, and X nucleons in the final state**

Interaction type	% age of fake events without cuts	% age of fake events with cuts
QE	25	28
RES	34	42

Table 6. **Percentage of fake events in GENIE, calculated as a difference of the total number of events before FSI and after FSI with condition on QE events as having $1\mu^-$, 0π, 1 proton and X neutrons in the final state and condition on RES events as having $1\mu^-$, 1π, and X nucleons in the final state**

Interaction type	% age of fake events without cuts	% age of fake events with cuts
QE	28	31
RES	37	47

the final state, no other type of hadrons are included in both the cases. In this definition of signal events, CCQE events may contain background

from 2p-2h processes and from RES processes where a single pion produced is absorbed in the nuclear matter. Similarly, RES events may contain a back-

ground from the QE processes, where a pion is produced in FSI.

The results of reconstructed energy are shown in Fig. 4 for NuWro and in Fig. 5 for GENIE, with and without detection threshold cuts. It is clear that, despite having a background, this definition of signal events gives better results for energy reconstruction. The percentages of fake events are shown in Tables 5 and 6, respectively,s for NuWro and GENIE. It is clear that the percentage of fake events, in this case, is much smaller than that in the previous case.

6. Summary

In the present work, we report an extensive analysis of nuclear effects on the energy reconstruction in DUNE. For this purpose, NuWro and GENIE simulation tools have been used, and CCQE and CCRES processes have been analyzed for 1 million events. The simulation is done for the DUNE Liquid Argon detector using the DUNE flux. It is observed that a major improvement in the energy reconstruction is obtained, when the condition for the selection of events for the final state is $1\mu^-$, 0π, exactly 1 proton and X neutrons for CCQE processes and $1\mu^-$, 1π and X nucleons for CCRES processes (Figs. 4 and 5), as compared to the condition $1\mu^-$ and exactly 1 proton for CCQE processes and $1\mu^-$, 1π and 1 nucleon for CCRES processes (Figs. 2 and 3). The correct reconstruction of neutrino energy is required for the correct estimation of neutrino oscillation parameters.

The percentage of fake events is also calculated for both the generators. It is clear from Tables 3 to 6 that the detector thresholds increase the percentage of fake events. In addition, the GENIE generator gives more fake events than NuWro due to the difference in nuclear transport models being used by these generators. For both generators, the percentage of fake events is lesser for QE events, which shows that, even for higher energy experiments such as DUNE, the energy reconstruction can be done in a better way from QE events. The uncertainties in the energy reconstruction show that it is critical to understand the neutrino-nucleus interactions, and we should have a good understanding of the hadronic physics involved in neutrino-nucleus interactions. The ignorance of nuclear effects and theoretical models can result in the inaccuracy in results. The wrong energy will be measured for those events for which the topology

of final-state particles is mistaken. Thus, to understand the role of these events, a high-quality Monte Carlo code is required.

1. Y. Farzan, M. Tortola. Neutrino oscillations and non-standard interactions. *Front. in Phys.* **6**, 10 (2018).
2. S. Nagu, J. Singh, J. Singh II, R.B. Singh. Nuclear effects and CP sensitivity at DUNE. *Adv. High Energy Phys.* **2020**, 5472713 (2020).
3. P. Adamson *et al.* (MINOS collaboration). A Study of muon neutrino disappearance using the Fermilab main injector neutrino beam. *Phys. Rev. D* **77**, 072002 (2008).
4. F.P. An *et al.* (Daya Bay collaboration). Observation of electron antineutrino disappearance at Daya Bay. *Phys. Rev. Lett.* **108**, 171803 (2012).
5. J.K. Ahn *et al.* (RENO collaboration). Observation of reactor electron antineutrino disappearance in the RENO experiment. *Phys. Rev. Lett.* **108**, 191802 (2012).
6. F.P. An *et al.* (Daya Bay collaboration). Improved measurement of electron antineutrino disappearance at Daya Bay. *Chin. Phys. C* **37**, 011001 (2013).
7. B. Abi *et al.* (DUNE collaboration). Deep underground neutrino experiment, far detector technical design report, volume I: introduction to DUNE. *JINST* **15** no.08, T08008 (2020).
8. B. Abi *et al.* (DUNE collaboration). Deep underground neutrino experiment, far detector technical design report, volume II: DUNE physics. arXiv:2002.03005 [hep-ex].
9. B. Abi *et al.* (DUNE collaboration). Deep underground neutrino experiment, far detector technical design report, volume III: DUNE far detector technical coordination. *JINST* **15** (8), T08009 (2020).
10. B. Abi *et al.* (DUNE collaboration). Deep underground neutrino experiment, far detector technical design report, volume IV: far detector single-phase technology. *JINST* **15** (8), T08010 (2020).
11. https://home.fnal.gov/~ljf26/DUNE2015CDRFluxes /NuMI_Improved_80GeV_StandardDP/g4lbne_ v3r2p4b_FHC_ND_globes_flux.txt.
12. D.A. Harris *et al.* (MINERvA collaboration). Neutrino scattering uncertainties and their role in long-baseline oscillation experiments. arXiv:hep-ex/0410005 [hep-ex].
13. P. Coloma, P. Huber, J. Kopp, W. Winter. Systematic uncertainties in long-baseline neutrino oscillations for large θ_{13}. *Phys. Rev. D* **87** (3), 033004 (2013).
14. P. Huber, M. Mezzetto, T. Schwetz. On the impact of systematical uncertainties for the CP violation measurement in superbeam experiments. *JHEP* **03**, 021 (2008).
15. M. Martini, M. Ericson, G. Chanfray. Neutrino energy reconstruction problems and neutrino oscillations. *Phys. Rev. D* **85**, 093012 (2012).
16. S. Naaz, A. Yadav, J. Singh, R.B. Singh. Effect of final state interactions on neutrino energy reconstruction at DUNE. *Nucl. Phys. B* **933**, 40 (2018).
17. M. Martini, M. Ericson, G. Chanfray. Neutrino energy reconstruction problems and neutrino oscillations. *Phys. Rev. D* **85**, 093012 (2012).

18. O. Lalakulich, K. Gallmeister, U. Mosel. Neutrino- and antineutrino-induced reactions with nuclei between 1 and 50 GeV. *Phys. Rev. C* **86**, 014607 (2012).

19. S. Nagu, J. Singh, J. Singh II, R.B. Singh. Impact of cross-sectional uncertainties on DUNE sensitivity due to nuclear effects. *Nuclear Physics B* **951**, 114888 (2020).

20. D. Drakoulakos *et al.* (MINERvA collaboration). Proposal to perform a high-statistics neutrino scattering experiment using a fine-grained detector in the NuMI beam. arXiv:hep-ex/0405002 [hep-ex].

21. J. Evans (MINOS collaboration). The MINOS experiment: Results and prospects. *Adv. High Energy Phys.* **2013**, 182537 (2013).

22. H. Chen *et al.* (MicroBooNE collaboration). Proposal for a new experiment using the booster and NuMI neutrino beamlines: MicroBooNE. *FERMILAB-PROPOSAL-0974*.

23. M.A. Acero *et al.* (NOvA collaboration). First measurement of neutrino oscillation parameters using neutrinos and antineutrinos by NOvA. *Phys. Rev. Lett.* **123** no.15, 151803 (2019).

24. K. Abe *et al.* (T2K collaboration). Constraint on the matter–antimatter symmetry-violating phase in neutrino oscillations. *Nature* **580** (7803), 339 (2020).

25. A. Bodek, J.L. Ritchie. Further studies of Fermi-motion effects in lepton scattering from nuclear targets. *Phys. Rev. D* **24**, 1400 (1981).

26. C.H. Llewellyn Smith. Neutrino reactions at accelerator energies. *Phys. Rept.* **3**, 261 (1972).

27. R. Bradford, A. Bodek, H.S. Budd, J. Arrington. A New parameterization of the nucleon elastic form-factors. *Nucl. Phys. B Proc. Suppl.* **159**, 127 (2006).

28. A. Bodek, S. Avvakumov, R. Bradford, H.S. Budd. Modeling atmospheric neutrino interactions: Duality constrained parametrization of vector and axial nucleon form factors. arXiv:0708.1827 [hep-ex].

29. K.M. Graczyk, D. Kielczewska, P. Przewlocki, J.T. Sobczyk. Axial form factor from bubble chamber experiments. *Phys. Rev. D* **80**, 093001 (2009).

30. D. Rein, L.M. Sehgal. Neutrino excitation of baryon resonances and single pion production. *Annals Phys.* **133**, 79 (1981).

31. H.R. Sharma, S. Nagu, J. Singh, R.B. Singh, B. Potukuchi. Study of pion production in ν_μ interactions on ^{40}Ar in DUNE using GENIE and NuWro event generators. arXiv:2204.05354 [hep-ph].

32. O. Lalakulich, U. Mosel, K. Gallmeister. Energy reconstruction in quasielastic scattering in the MiniBooNE and T2K experiments. *Phys. Rev. C* **86**, 054606 (2012).

33. J. Singh, S. Nagu, J. Singh II, R.B. Singh. Quantifying multinucleon effect in argon using high-pressure TPC. *Nuclear Physics B* **957**, 115103 (2020).

34. L. Alvarez-Ruso *et al.* (NuSTEC collaboration). NuSTEC white paper: status and challenges of neutrino-nucleus scattering. *Prog. Part. Nucl. Phys.* **100**, 1 (2018).

35. A.M. Ankowski, O. Benhar, P. Coloma, P. Huber, C.M. Jen, C. Mariani, D. Meloni, E. Vagnoni. Comparison of the calorimetric and kinematic methods of neutrino energy reconstruction in disappearance experiments. *Phys. Rev. D* **92** (7), 073014 (2015).

36. A.M. Ankowski, P. Coloma, P. Huber, C. Mariani, E. Vagnoni. Missing energy and the measurement of the CP-violating phase in neutrino oscillations. *Phys. Rev. D* **92** (9), 091301 (2015).

37. K. Abe *et al.* (T2K collaboration). The T2K experiment. *Nucl. Instrum. Meth. A* **659**, 106 (2011).

38. D. Meloni, M. Martini. Revisiting the T2K data using different models for the neutrino–nucleus cross sections. *Phys. Lett. B* **716**, 186 (2012).

39. D.G. Michael, P. Adamson, T. Alexopoulos, W.W.M. Allison, G.J. Alner, K. Anderson, C. Andreopoulos, M. Andrews, R. Andrews, C. Arroyo. The magnetized steel and scintillator calorimeters of the MINOS experiment. *Nucl. Instr. Methods in Phys. Res. Sec.* **596**, 190 (2008).

40. D.S. Ayres *et al.* (NOvA collaboration). NOvA: Proposal to build a 30 kiloton off-axis detector to study $\nu_\mu \to \nu_e$ oscillations in the NuMI beamline. arXiv:hep-ex/0503053 [hep-ex].

41. C. Adams *et al.* (LBNE collaboration). The long-baseline neutrino experiment: exploring fundamental symmetries of the universe. arXiv:1307.7335 [hep-ex].

42. R. Acciarri *et al.* (DUNE collaboration). Long-baseline neutrino facility (LBNF) and deep underground neutrino experiment: conceptual design report, volume 2: The physics program for DUNE at LBNF. arXiv:1512.06148 [physics.ins-det].

Х.Р. Шарма, С. Нагу,
Дж. Сингх, Р.Б. Сингх, Б. Потукучі

КІЛЬКІСНА ОЦІНКА ЕФЕКТІВ ВЗАЄМОДІЇ
У КІНЦЕВОМУ СТАНІ ПРИ ВИЗНАЧЕННІ ЕНЕРГІЇ
В ЕКСПЕРИМЕНТАХ ІЗ НЕЙТРИНО ГЛИБОКО
ПІД ЗЕМНОЮ ПОВЕРХНЕЮ

В нейтрино-ядерних взаємодіях частинки, що утворюються в первинній вершині, можуть відрізнятися від частинок, які спостерігаються у кінцевому стані. Це трапляється завдяки ефекту взаємодії частинок у кінцевому стані під час їхнього руху крізь ядерну матерію до детектора. В цій роботі виконано реконструкцію енергії для квазіпружного та резонансного розсіювань на заряджених струмах (КРЗС та РРЗС) з використанням калориметрії та програм NuWro і GENIE для моделювання. Розраховано відсотки помилкових подій для КРЗС і РРЗС. Ці відсотки в обох випадках і для обох програм є більшими, ніж 50%, якщо прийняти умову, що частинки в кінцевому стані ті самі, що утворилися в первинній вершині. Відновлене значення енергії та кількість помилкових подій можуть змінюватися в залежності від визначення сигнальних подій. Це впливає на результати вимірювання параметрів осциляцій в експериментах з довгою базою, таких як експерименти з нейтрино глибоко під земною поверхнею.

К л ю ч о в і с л о в а: взаємодія в кінцевому стані, експерименти з нейтрино глибоко під земною поверхнею, помилкові події, реконструкція енергії.